Chemical and Process Engineering: New Frontiers, 2025, 46(3), e97
DOI: 10.24425/cpe.2025.153682

# Transport properties of glassy polymer membrane after exposure to $H_2S$

Aleksandra Janusz-Cygan[1*], Grzegorz Wiciak[2], Katarzyna Janusz-Szymańska[2], Marek Tańczyk[1]

[1] Polish Academy of Sciences, Institute of Chemical Engineering, Bałtycka 5, 44-100 Gliwice, Poland
[2] Silesian University of Technology, Department of Power Engineering and Turbomachinery, Konarskiego 18, 44-100 Gliwice, Poland

*** Corresponding author, e-mail:** ajcygan@iich.gliwice.pl

**Article info:**
Received: 03 June 2025
Revised: 30 June 2025
Accepted: 10 July 2025

**Abstract**
Membrane processes continue to attract significant interest, as reflected in the growing number of studies focused on the development of innovative membrane materials. Novel membranes are frequently designed for specific separation processes, in which they demonstrate enhanced transport properties and improved resistance to fouling. In this study, a methodology was proposed to evaluate the transport properties of novel membrane materials with respect to their resistance to hydrogen sulfide, a common contaminant in biogas. To this end, the permeance, solubility, and diffusivity of $CH_4$, $CO_2$, $N_2$, and $O_2$ were experimentally determined both before and after exposure of a glassy polyimide membrane to hydrogen sulfide. Exposure to $H_2S$ resulted in a reduction of both permeation and diffusivity coefficients for all investigated gases. It was also observed that hydrogen sulfide exposure did not significantly affect the overall gas solubility. Notably, only for $CO_2$ an increase in gas mobility within the fractional free volume was detected, whereas the mobility of the remaining gases was effectively diminished. To describe the solubility and diffusivity behavior of the gases in the glassy polyimide membrane, the Dual Mode Sorption and partial immobilization models were applied. The parameters of the *DMS* model were determined based on gravimetric sorption experiments.

**Keywords**
gas separation, polyimide-based membrane, glassy polymer, Dual Mode Sorption model, partial immobilization model

## 1. INTRODUCTION

The current challenging geopolitical situation worldwide, the European Green Deal, and the associated Methane Emissions Reduction Strategy have a direct impact on the biomethane market. The rapid development of biomethane installations can support both the increasingly important goal of reducing dependence on external supplies of natural gas and energy, and the mitigation of climate change by replacing fossil fuels with new, low-emission energy sources. Biogas plants that use agricultural waste to produce biofertilizers and biogas – a renewable energy carrier – also align with the circular economy policy.

Biogas is a by-product of the biological decomposition of organic matter (such as manure, plant and animal waste, and municipal sewage). The quantity and quality of the biogas produced are significantly influenced by both the amount and quality of the feedstock subjected to fermentation, as well as the process conditions. The main components of biogas include methane and carbon dioxide, which are present in quantities of approximately 45–70% and approximately 25–45% by volume, respectively (Janusz-Cygan et al., 2021; Tomczak et al., 2024; Werkneh, 2022). Agricultural biogas may also contain small amounts of nitrogen and oxygen. The physicochemical similarity of biogas to natural gas makes it a potential substitute, provided that it is standardized – i.e. upgraded to biomethane with a stable calorific value comparable to that of natural gas by reducing the concentration of $CO_2$ and other trace impurities. A significant issue is the presence of trace amounts of hydrogen sulfide ($H_2S$) in biogas, as water vapor contained in the gas forms corrosive compounds with $H_2S$. Failure to meet biomethane quality requirements can lead to increased operational costs, accelerated equipment wear, intensified corrosion, and, over time, equipment failure (Fajrina et al., 2023; Katariya and Patolia, 2023; Pudi et al., 2022). The permissible level of contaminants in biomethane depends on its intended use: biomethane used in vehicle engines may typically contain 50 to 100 ppm of $H_2S$, while biomethane injected into the natural gas grid must contain less than 5 ppm of $H_2S$ (Ahmad et al., 2020; Harrigan et al., 2020; Pudi et al., 2022).

Membrane processes in the context of biogas upgrading have already found practical application in large-scale installations with capacities of several hundred $m^3/h$ of biogas, operating at pressures exceeding 1 MPa (Air Liquide; PRISM®GreenSep; SEPURAN®Green; UBE $CO_2$ separator). Despite the widespread use of membrane technology,

intensive research is still ongoing into innovative membrane materials that would exhibit improved transport properties and greater resistance to contaminants.

One of the most important challenges for new materials is to increase their resistance to acidic gases such as $CO_2$ and $H_2S$, which can cause membrane swelling or plasticization. To minimize these effects, various modification polymer strategies are employed, including polymer blending, crosslinking and thermal rearrangement (Cai et al., 2025; Harrigan et al., 2020; Sidhikku Kandath Valappil et al., 2021; Suleman et al., 2016; Xu et al., 2022). A more promising method is the combination of polymeric and inorganic materials as mixed matrix membranes (Ahmad et al., 2020; Mashhadikhan et al., 2024; Polak and Szwast, 2022; Pudi et al., 2022).

New membranes are subjected to diffraction, thermal, mechanical, and sorption tests (Ahmad et al., 2020; Harrigan et al., 2020). When assessing resistance to swelling and plasticization, membranes are typically tested for $CO_2$ removal, since $H_2S$ is a toxic gas. As a result, the available literature on these materials provides very limited information regarding their resistance to trace contaminants present in biogas, such as hydrogen sulfide. Only a few researchers have undertaken studies involving this gas. In another work (Ahmad et al., 2020) compared the permeability of $H_2S$ in pure polyimide and in a mixed matrix polyimide. He used a gas mixture composed of 65% $CH_4$ – 30% $CO_2$ – 5% $H_2S$. His findings indicated that the mixed matrix membrane exhibited greater resistance to plasticization.

The study thus presents a conceptual methodology enabling a comprehensive and systematic assessment of the impact of hydrogen sulfide present in biogas on the transport properties of novel membrane materials. For this purpose, the permeability of the main biogas components ($CH_4$ and $CO_2$) as well as the most common impurities found in agricultural biogas ($N_2$ and $O_2$) were determined before and after exposing a glassy polyimide membrane to hydrogen sulfide. The research employed a stable commercial membrane used in the UBE UMS-A5 module. To gain a more complete understanding of the influence of hydrogen sulfide on the membrane, the total solubility of all investigated gases in the membrane was determined using the gravimetric method. The measurements were conducted for $CO_2$, $CH_4$, $N_2$, and $O_2$ using a pristine membrane sample. This sample was then exposed to a gas mixture containing 25 ppm $H_2S$ in $N_2$, after which gravimetric measurements were repeated for all gases. Using the Dual Mode Sorption model (*DMS*), the contributions of each gas to sorption in the polymer matrix and their adsorption within the fractional free volume (*FFV*) of the glassy polymer were also determined. Based on the solubility of $CO_2$, $CH_4$, $O_2$, and $N_2$ calculated from the *DMS* model and the experimentally determined permeability of these gases, their diffusion coefficients were calculated for the tested polyimide membrane sample both before and after $H_2S$ exposure. The partial immobilization model was employed to determine these diffusion coefficients.

## 2. MODELS, MATERIALS AND METHODS

### 2.1. Dual Mode Sorption (DMS) model and partial immobilization model

Gas transport in dense polymer membranes is described by the solution-diffusion model (Wijmans and Baker, 1995), according to which permeability, $P$, is defined as the product of solubility, $S$, and the diffusion coefficient, $D$:

$$P_i = S_i D_i = Q_i \delta_M \tag{1}$$

In this equation, permeability is related to the gas permeance, $Q$, and the membrane thickness, $\delta_M$. The value of $Q$ can be directly determined from the mass flux and the pressure difference across the membrane, as measured in permeation experiments. The ratio of the permeability coefficients of two gases, denoted as gas-$i$ and gas-$j$, is referred to as selectivity, $\alpha_{ij}$, which is a key parameter for evaluating membrane separation performance:

$$\alpha_{ij} = \frac{P_i}{P_j} = \left(\frac{S_i}{S_j}\right)\left(\frac{D_i}{D_j}\right) = \alpha_{S_{ij}} \alpha_{D_{ij}} \tag{2}$$

When the parameters in Equation (2) refer to pure gases, the resulting value is referred to as the ideal selectivity.

The sorption of gases in glassy polymers is typically described using the Dual Mode Sorption model, which combines Henry's law sorption and Langmuir-type sorption. This model accounts for the presence of molecules dissolved in the polymer matrix, which can diffuse according to the concentration gradient, $C_D$, as well as molecules trapped in microvoids or specific adsorption sites within the polymer, $C_H$. The *DMS* model, developed and based on the work by (Tsujita, 2003) is illustrated conceptually in Figure 1.

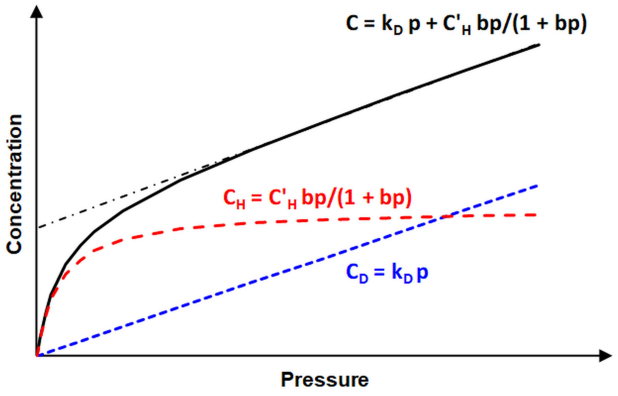


Figure 1. Gas sorption isotherm in glassy polymers (*DMS* model).

According to the *DMS* model, gas sorption isotherms in glassy polymers reveal nonlinearity in their initial (low-pressure) region. The total gas concentration, $C$, in a glassy polymer membrane is then expressed as follows:

$$C_i = C_{D_i} + C_{H_i} = k_{D_i} p_i + C'_{H_i} \frac{b_i p_i}{1 + b_i p_i} \tag{3}$$

where $k_D$ is Henry's solubility coefficient, $p$ is the gas pressure, $c'_H$ is the Langmuir saturation constant, and $b$ is the Langmuir affinity coefficient.

The solubility of the gas in the membrane can be expressed as:

$$S_i = \frac{C_i}{p_i} = k_{D_i} + C'_{H_i} \frac{b_i}{1 + b_i p_i} \tag{4}$$

Assuming the validity of Fick's law in both the solution-diffusion and Dual Mode Sorption models, the diffusion coefficient can be derived as (Tsujita, 2003):

$$D_i = D_{D_i} \left[ \frac{1 + \frac{F_i K_i}{(1 + b_i p_i)^2}}{1 + \frac{K_i}{(1 + b_i p_i)^2}} \right] = D_{D_i} \left[ \frac{(1 + b_i p_i)^2 + F_i K_i}{(1 + b_i p_i)^2 + K_i} \right] \tag{5}$$

where $K$ is a dimensionless parameter describing the relationship between Langmuir and Henry sorption:

$$K_i = \frac{C'_{H_i} b_i}{k_{D_i}} \tag{6}$$

The dimensionless constant $F$ is the ratio of the diffusion coefficient in the Langmuir mode species, $D_H$ to the diffusion coefficient in the Henry mode species, $D_D$:

$$F_i = \frac{D_{H_i}}{D_{D_i}} \tag{7}$$

The set of Equations (5)–(7) is referred to in the literature (Hayashi et al., 1999; Tańczyk et al., 2025; Tsujita, 2003), as well as in the present work, as the partial immobilization model.

The parameters of the Dual Mode Sorption model for the sorption of individual gases ($CO_2$, $CH_4$, $O_2$, and $N_2$) in the polyimide membrane sample were determined based on the obtained experimental isotherms. The individual coefficients of the *DMS* model were determined using the least squares method, with Equation (4) used as the fitting basis. The quality of the fit was assessed using the average relative error (*ARE*) and the standard error of the estimate (*SEE*) (Ricci and De Angelis, 2019), which were defined as follows:

$$ARE = \frac{\sum_j \frac{|y_{j_{exp}} - y_{j_{calc}}|}{y_{j_{exp}}}}{n} \tag{8}$$

$$SEE = \sqrt{\frac{\sum_j \left(y_{j_{exp}} - y_{j_{calc}}\right)^2}{n - r}} \tag{9}$$

where $y_{j_{exp}}$ is the *j-th* experimental point, $y_{j_{calc}}$ is the point calculated by the *DMS* model, $n$ is the number of experimental points used in the regression, and, $r$ is the number of model parameters.

## 2.2. Membrane module and gases

In the gas permeability studies of biogas components, a hollow fiber membrane module of the UMS-A5 type, manufactured by UBE (Japan), was used. The active layer of the membrane is made of modified polyimide. The maximum operating parameters of this module are 333 K and 10 bar. For the sorption experiments, individual membrane fibers were used, which were cut into pieces approximately 2 mm in length. In this way, a sample with an initial mass of 103 mg was prepared.

In the permeation experiments, all pure gases ($CO_2$, $CH_4$, $O_2$ and $N_2$) of technical grade purity and a gas mixture containing 100 ppmv of $H_2S$ in $N_2$ supplied by Messer Polska, were used. In the sorption experiments, gases from various suppliers (Messer, Siad, and Air Liquide) with high purity levels (99.95% to 99.9999%) were used.

## 2.3. Permeation experiments

Permeation experiments with pure gases were carried out using a dedicated test setup, the schematic diagram of which is shown in Figure 2, while a detailed description is provided in (Wiciak et al., 2023) work.

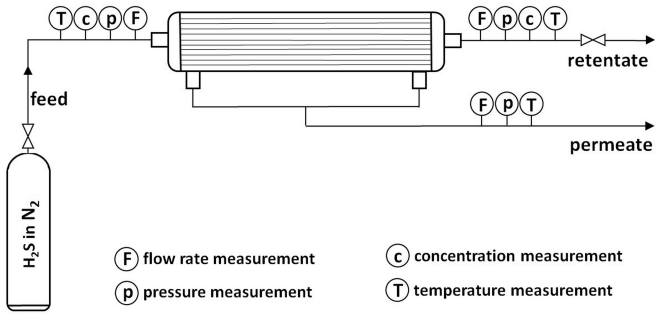


Figure 2. The experimental setup.

The experimental setup was centered around a UBE UMS-A5 module incorporating a membrane fabricated from glassy polyimide. Pure gases ($CO_2$, $CH_4$, $O_2$, and $N_2$), as well as a gas mixture (100 ppmv $H_2S$ in $N_2$), were sequentially introduced into the lumen side of the membrane module. Upon contact, the gases were partially absorbed into the polymer matrix and subsequently diffused across the membrane to the shell side, where they were collected as permeate. The non-permeating fraction was discharged at the module outlet as retentate.

During the permeation experiments, flow rate, pressure, and temperature were monitored and controlled in the feed, retentate, and permeate streams. Flow rates were measured using Aalborg DFM27 (0–500 $cm^3$/min) and GFM17 (0–200 $cm^3$/min) flow meters, each with an accuracy of ±1% of full scale. Pressures were measured using Cole–Parmer Series P pressure transducers with a precision of 6.9 mbar. Temperatures were recorded using a Cole–Parmer temperature transmitter, which provided an accuracy of ±0.1 K. In experiments involving the gas mixture containing 100 ppm of $H_2S$,

the hydrogen sulfide concentration in the retentate stream was additionally measured every 5 minutes using a portable Nanosens DP-28 analyzer. The measurement range of this device is 0–5000 ppm $H_2S$, with an accuracy of ±50 ppm.

Each day after testing, the membrane installation was purged with pure nitrogen. The purging was conducted for approximately 90 minutes by passing nitrogen at a flow rate of 300 $cm^3$/min under a pressure of 4.4 bar.

Permeation experiments were carried out at a constant feed gas flow rate of 300 $cm^3$/min and a constant temperature of approximately 294–295 K, while the feed pressure was varied in the range of 1–7 bar. The different feed pressure ranges result from the different permeation rates of the individual gases.

To evaluate the influence of hydrogen sulfide on the transport properties of the membrane, permeation experiments with pure gases were performed both before and after membrane exposure to $H_2S$.

### 2.4. Sorption experiments

Sorption isotherms for individual gases ($CO_2$, $CH_4$, $O_2$ and $N_2$) as well as for the gas mixture containing 25 ppm $H_2S$ in $N_2$) were determined based on gravimetric measurements performed using a microbalance (IGA003, Hiden Isochema Ltd, UK). The measurement resolution of the microbalance is 0.2 µg. To eliminate the influence of ambient temperature, the microbalance was fully thermostated, with temperature fluctuations not exceeding ±0.2 K. The measurements were carried out in static mode, i.e., the sample container was filled with gas until the desired pressure was reached. Subsequently, the gas inlet was closed, and the system was allowed to reach equilibrium. The IGA microbalance has been described in detail in the work by (Bahadur et al., 2015).

Prior to the measurements, the sample was outgassed in situ at 523 K under vacuum for 24 hours and then its density was determined. The sample was weighed in a helium atmosphere. Measurements were taken after each pressure step of 500 mbar in the range of 2–17.5 bar. The temperature was maintained at a constant level of 293 K. The sample density determined in this way was equal to 1.40 g/$cm^3$. The sample was degassed before each gas change.

Sorption isotherms of gases ($CO_2$, $CH_4$, $O_2$, $N_2$ and 25 ppm $H_2S$ in $N_2$) at the given temperature were determined by stepwise pressure variation in the range from 0 to 17.5 bar. The ramp rate in pressure in the IGA chamber was 200 mbar/min. Once the reactor pressure reached the set maximum value, the depressurization process was initiated. For each isotherm, one pressurization cycle and one depressurization cycle were carried out. The measurement of a given isotherm point was considered complete when the sample mass reached 99.8% of the predicted asymptotic value, or when the measurement time exceeded 40 minutes for $CO_2$ and 30 minutes for other gases.

In order to evaluate the effect of hydrogen sulfide on the transport properties of the membrane, sorption measurements of pure gases were conducted both before and after the membrane's exposure to $H_2S$.

## 3. RESULTS AND DISCUSSION

### 3.1. Permeation experiments

The results of the permeation process tests in the UBE UMS-A5 module for a gas mixture containing 100 ppm $H_2S$ in $N_2$ are presented graphically in Figure 3.

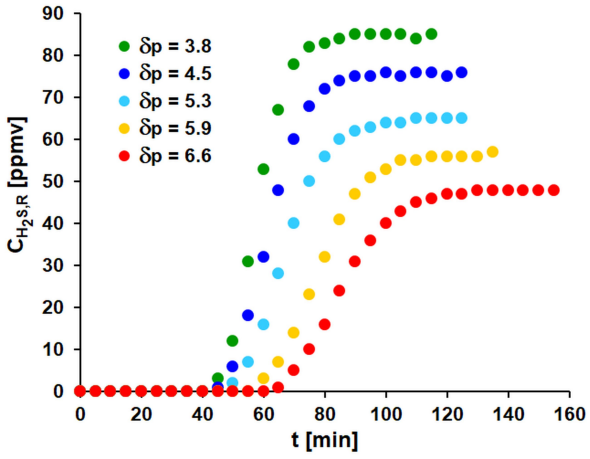


Figure 3. Time-dependent changes in $H_2S$ concentration in the retentate for different pressure ratio.

It can be observed that for the first 40 minutes of operation, only pure nitrogen is detected on the retentate side, with no trace of hydrogen sulfide. After this period $H_2S$ begins to appear in the retentate stream. It was found that the time at which hydrogen sulfide appears on the retentate side is strictly dependent on the transmembrane pressure ratio – the lower the pressure ratio ($\delta p = p_Z/p_P$), the earlier $H_2S$ is detected. For example, for $\delta p = 3.8$, hydrogen sulfide appears on the retentate side after approximately 45 minutes of operation. After this time, the $H_2S$ concentration increases monotonically until it reaches a steady-state value of 85 ppmv, which occurs after about 85 minutes of operation. Simultaneously, the $H_2S$ concentration in the retentate stream decreases as the pressure ratio increases. This observed phenomenon suggests that the membrane material became saturated with hydrogen sulfide, and the driving force of the process (in this case, the transmembrane partial pressure difference) was too low for effective transport of $H_2S$ across the membrane.

Due to the very low permeate flow rate and the resulting limitations of the analyzer used to measure $H_2S$ concentration, measurements of hydrogen sulfide concentration could only be performed on the retentate side. It is worth noting that in all experiments, the pressure on the permeate side was atmospheric; therefore, an increase in the pressure ratio was solely due to an increase in the feed pressure.

As previously mentioned, after each series of experiments, the membrane installation was purged with pure nitrogen. During this process, a change in the hydrogen sulfide concentration in the retentate stream was observed, as shown in Figure 4.

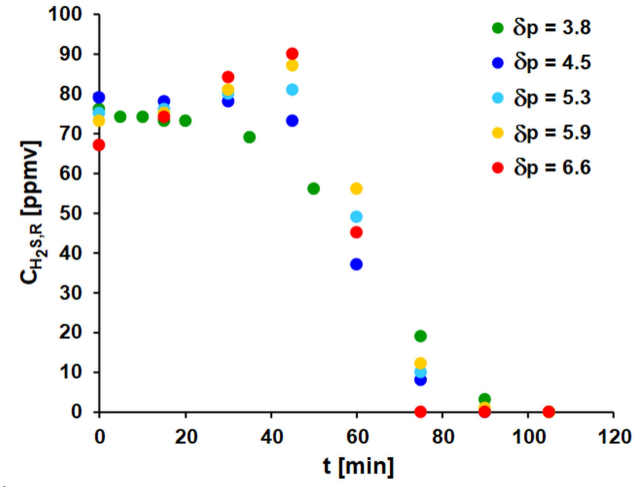


Figure 4. Membrane flushing.

It was found that during the first 30 minutes of purging the installation, the $H_2S$ concentration level remained constant for the lowest pressure ratio, while with increasing $\delta p$, the $H_2S$ concentration in the retentate increased to a maximum value that exceeded the levels observed during the permeation tests. After reaching the maximum, the hydrogen sulfide concentration in the retentate rapidly decreased, reaching zero after approximately 90 minutes. The results indicate that hydrogen sulfide, as a highly condensable and polar gas (Ahmad et al., 2020; Soroodan Miandoab et al., 2021; Pudi et al., 2022), accumulates in the void spaces of the glassy polymer membrane at higher feed pressures, making it more difficult to remove (Soroodan Miandoab et al., 2021).

In order to assess the impact of hydrogen sulfide on the transport properties of the membrane, permeation tests with pure gases were carried out before and after membrane exposure to $H_2S$. During the tests, permeate flow rates, $F_{iP}$, were determined for various feed gas pressures, at a constant and controlled feed flow rate. Following membrane exposure to hydrogen sulfide, the system was purged with carbon dioxide and nitrogen for approximately 200 hours until a stable permeate flow was achieved under constant process conditions. The obtained results are presented graphically in Figure 5. Permeation tests after membrane exposure to $H_2S$ were repeated three times, and the standard deviation for each measurement is indicated on the corresponding plots. The error bars are also given below the figures because the mean standard deviation is small and therefore difficult to see.

It can be observed that for each gas, the permeate flow rate increases linearly with the increase in transmembrane pressure difference, and the plot passes through the origin of the coordinate system, which confirms the correctness of the performed measurements. It was also found that for each gas, the permeate flow rate decreased by 30%–40% after membrane exposure to hydrogen sulfide. Therefore, it can be stated that the transport properties of the tested membrane changed after its exposure to $H_2S$.

According to Equation (10) describing the gas flux through the membrane:

$$F_{Pi} = AQ_i\Delta p_i \tag{10}$$

where $A$ is the membrane area and $\Delta p_i$ denotes the transmembrane pressure difference, the permeation coefficients, $Q_i$, of individual gases can be easily calculated. The only unknown here is the membrane area, as commercial membrane module suppliers do not disclose this value. However, to determine the permeation of individual gases, the membrane area of the tested module was assumed to be 167 $cm^2$, according to (Wiciak et al., 2021). The obtained permeation coefficients are presented in Table 1 and Figure 6.

The points in Figure 6 correspond to the experimentally determined permeation coefficients (dashed lines are added for better visibility). It can be observed that the permeation coefficients have lower values for all gases after the membrane's exposure to hydrogen sulfide. For gas permeation measurements before membrane exposure to $H_2S$, the permeation coefficients of all tested gases are constant and independent of the feed pressure. However, after exposure membrane to $H_2S$, only the permeation coefficients of $CO_2$ and $CH_4$ remain constant and pressure-independent, whereas the permeation coefficients of $O_2$ and $N_2$ increase with rising pressure.

The presented results show that carbon dioxide permeates best through the polyimide membrane, while methane permeates the least. This conclusion applies to the transport properties of the tested membrane both before and after its exposure to hydrogen sulfide. As can be observed, the permeabilities of individual gases in the glassy polyimide membrane deteriorated by approximately 30–42% after the membrane was exposed to hydrogen sulfide.

It is worth noting that although membrane exposure to hydrogen sulfide led to a decline in gas permeabilities, the ideal selectivity coefficients increased by 3.6% and 15.4% for $O_2/N_2$) and $CO_2/CH_4$, respectively. Similar conclusions, based on literature data analysis, were presented in (Kadirkhan et al., 2022; Suleman et al., 2016). Considering the fact that acidic gases accelerate the aging of glassy polymers (Pudi et al., 2022), it can be assumed that the observed decrease in permeability accompanied by an increase in selectivity is indicative of this phenomenon.

## 3.2. Solubility of pure $CO_2$, $CH_4$, $O_2$ and $N_2$

To gain a more comprehensive understanding of the influence of hydrogen sulfide on the membrane, the total solubility of all tested gases in the polyimide membrane sample was

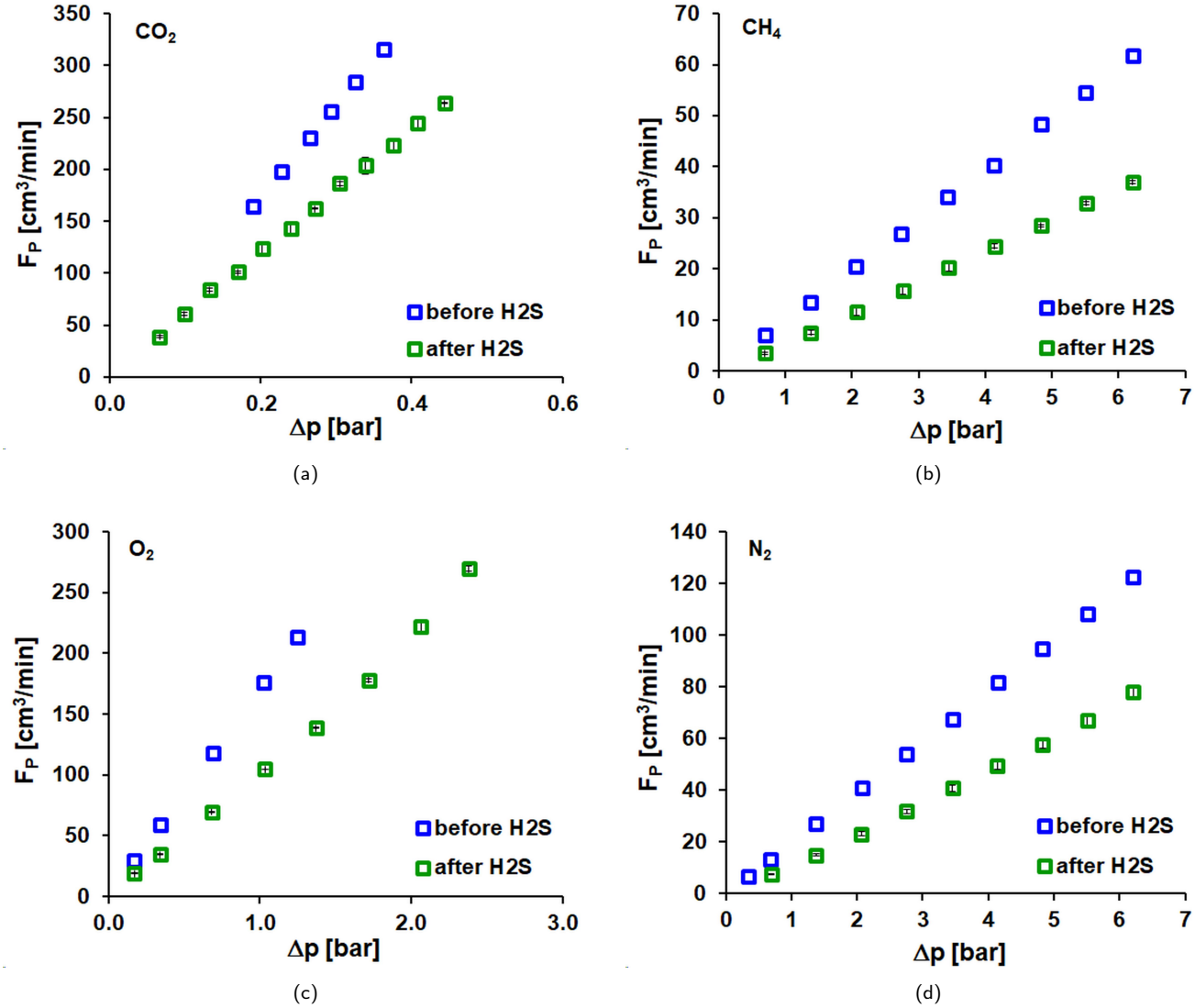


Figure 5. Volumetric flux of permeate vs. pressure drop for (a) $CO_2$, (b) $CH_4$, (c) $O_2$ and (d) $N_2$ at ambient temperature. Standard deviation after $H_2S$: $F_{CO2} = \pm 2.95$, $F_{CH4} = \pm 0.46$, $F_{O2} = \pm 1.24$ and $F_{N2} = \pm 1.23$.

Table 1. The transport properties of the membrane before and after exposure to $H_2S$ at ambient temperature

| Gas | $Q$ [cm$^3$(STP)/(cm$^2$·s·bar)] before $H_2S$ | $Q$ [cm$^3$(STP)/(cm$^2$·s·bar)] after $H_2S$ |
|---|---|---|
| $CO_2$ | $8.04 \times 10^{-2}$ for $p_z = 1.2 - 1.4$ bar | $5.55 \times 10^{-2}$ for $p_z = 1.2 - 1.4$ bar |
| $CH_4$ | $9.16 \times 10^{-4}$ for $p_z = 1,7 - 7.2$ bar | $5.48 \times 10^{-4}$ for $p_z = 3 - 7.2$ bar |
| $O_2$ | $1.59 \times 10^{-2}$ for $p_z = 1.2 - 2.2$ bar | $1.05 \times 10^{-2}$ for $p_z = 3.4$ bar |
| $N_2$ | $1.82 \times 10^{-3}$ for $p_z = 1.6 - 7.2$ bar | $1.16 \times 10^{-3}$ for $p_z = 7.2$ bar |

determined using a gravimetric method. An example of the sorption kinetics of pure gases ($CO_2$, $CH_4$, $O_2$, and $N_2$) in the polyimide-based membrane at 293 K, with a pressure change from 5 to 7.5 bar, is shown in Figure 7. The individual curves illustrate the increase in sample mass over time, which results from gas sorption caused by the pressure change. It can be observed that for all gases, the total mass increase of the sample is reached after about 13 minutes (simultaneously with the pressure increase from 5 to 7.5 bar). After this time, the sample mass remains constant, indicating that sorption equilibrium has been achieved. The changes in sample mass are relatively small, amounting to 0.1 mg for $CH_4$ and $O_2$, and 0.04 mg for $N_2$ and the $N_2 + 25$ ppmv $H_2S$ mixture. However, these changes significantly exceed the measurement resolution of the microbalance (0.2 µg).

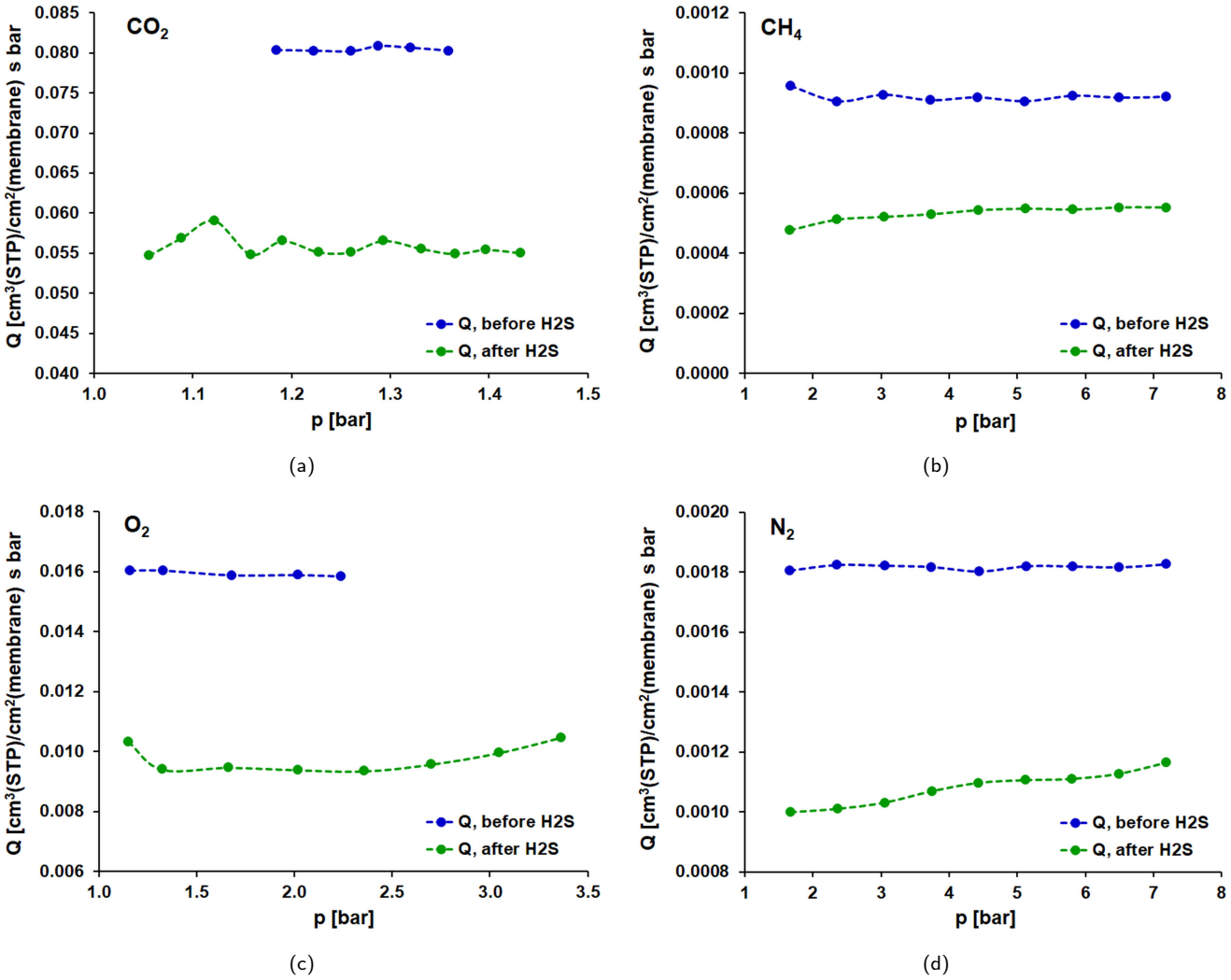


Figure 6. Permeation coefficients vs. feed pressure for (a) $CO_2$, (b) $CH_4$, (c) $O_2$ and (d) $N_2$ at ambient temperature. Standard deviation before $H_2S$: $Q_{CO2} = \pm 0.0003$, $Q_{CH4} = \pm 0.000008$, $Q_{O2} = \pm 0.0001$ and $Q_{N2} = \pm 0.000008$. Standard deviation after $H_2S$: $Q_{CO2} = \pm 0.0007$, $Q_{CH4} = \pm 0.00001$, $Q_{O2} = \pm 0.0002$ and $Q_{N2} = \pm 0.00004$.

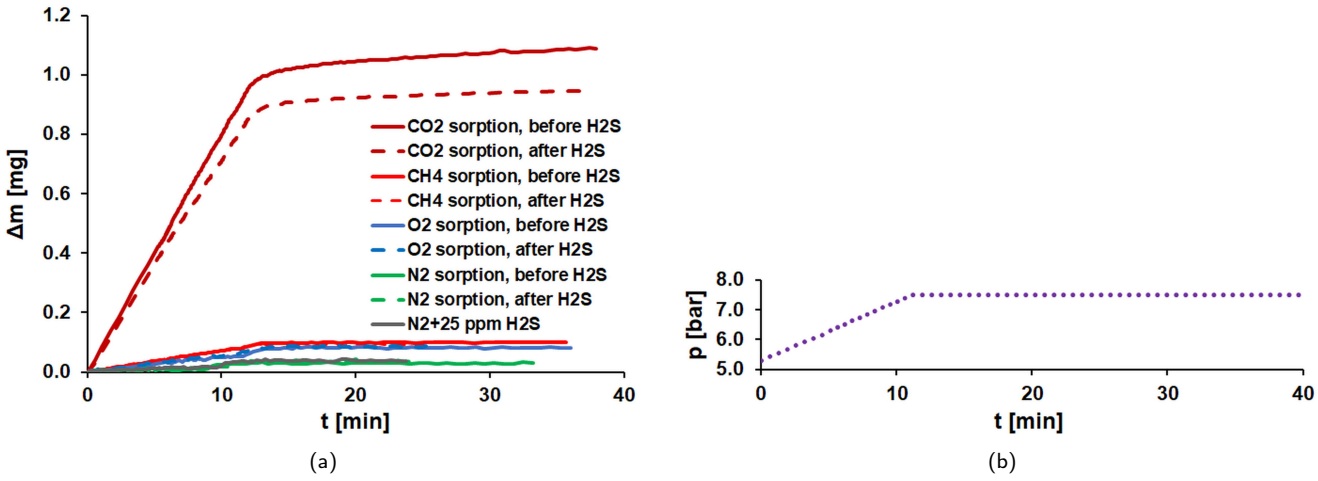


Figure 7. Mass changes due to sorption of pure gases ($CO_2$, $CH_4$, $O_2$ and $N_2$) in the polyimide-based membrane from UBE's UMS-A5 module before and after exposure of the membrane to $H_2S$ corresponding to the sorption equilibria at 293 K and pressure range of 5–7.5 bar.

Only in the case of $CO_2$, after an initial rapid mass increase of about 1.1 mg, a slight but monotonic mass gain continues until the end of the measurement at a given isotherm point. This steady increase in sorption capacity may be caused by polymer swelling due to $CO_2$. It is worth noting that for the membrane after exposure to $H_2S$, the $CO_2$ sorption kinetics trend was preserved although the amount of adsorbed carbon dioxide decreased. No similar phenomenon was observed for the other gases.

The lack of sorption equilibrium for $CO_2$ is also visible on the graph showing carbon dioxide solubility in the polyimide membrane (Figure 8). It can be assumed that the observed hysteresis (desorption points lying above sorption points) is related to the presence of another phenomenon that visibly accompanies physical sorption/desorption. Most likely, $CO_2$ condensation occurred in the polymer micropores, in which case the desorption kinetics is significantly slower than that of sorption.

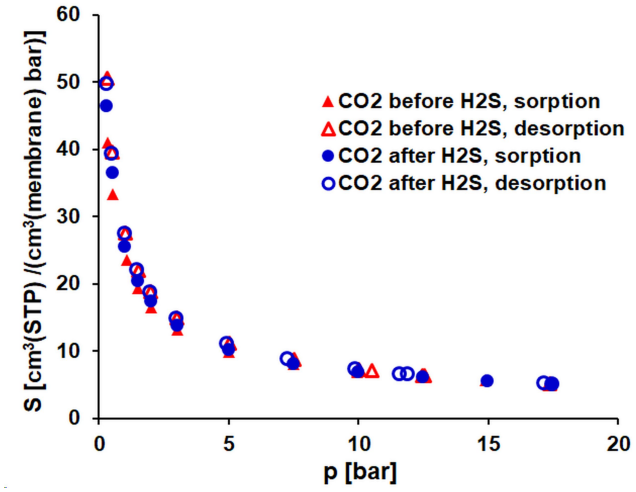


Figure 8. Experimental solubility of $CO_2$ in the polyimide-based membrane from UBE's UMS-A5 module before and after exposure of the membrane to $H_2S$ at 293 K.

Both phenomena – $CO_2$ condensation in glassy polymers and their swelling under high $CO_2$ pressure – are well documented in the literature (Houben et al., 2021; Tiwari et al., 2017). These effects are unfavorable for the membrane-based separation of gas mixtures containing carbon dioxide, such as biogas. $CO_2$ condensation within the fractional free volume ($FFV$) of a glassy polymer may hinder the desorption of $CO_2$ from this region, consequently limiting the overall membrane permeability to this gas (Kadirkhan et al., 2022). On the other hand, polymer swelling deteriorates membrane selectivity by facilitating the transport of gas mixture components being separated from $CO_2$ (e.g., methane in the case of biogas) (Kadirkhan et al., 2022; Ricci et al., 2022; Suleman et al., 2016).

In industrial applications, membrane swelling should be avoided, as it would render the separation properties of the membrane unstable and unpredictable. In practice, commercial membrane systems are designed for specific processes and well-defined operating conditions. Only under such circumstances can the expected service lifetime of the membrane system (e.g., 8–12 years) be guaranteed. Therefore, this aspect should be taken into account when developing new membrane materials.

To verify whether the sample underwent any permanent changes as a result of its exposure to hydrogen sulfide, density measurements were repeated after the gravimetric sorption tests were completed. The same sample density was obtained. It can therefore be concluded that exposure to $H_2S$ did not cause any macroscopically detectable changes in the tested polymer. The sorption isotherms of all gases are presented in Figure 9.

It can be observed that the solubility of carbon dioxide in the tested membrane is strongly nonlinear and several times higher than that of all the other gases. The largest differences are observed at low pressures. This conclusion applies to the gas solubility in the membrane both before and after the sample's exposure to hydrogen sulfide. At the same time, the solubility of $CO_2$ in the membrane increased at the lowest pressures following $H_2S$ exposure. However, such low pressures are not typically used in real membrane processes. Similar solubility behavior of $CO_2$, $CH_4$, $O_2$, and $N_2$ in other polyimide-based materials has been reported in (Baker and Low, 2014; ; Hu et al., 2003; Ricci et al., 2022; Scholes et al., 2010).

For all the isotherms, discussed above, including the one in which hysteresis was observed, the sample returned to its original state after regeneration, both in terms of its initial mass and sorption capacity for all gases. Both identified phenomena – namely $CO_2$ condensation in the fractional free volume and membrane swelling – are therefore reversible within the range of pressures and temperatures applied in the study. This is consistent with the widely reported view in the available literature regarding the impact of carbon dioxide on the state of glassy membranes (Ahmad et al., 2020; Bos et al., 1999; Kadirkhan et al., 2022; Scholes et al., 2010).

The sorption isotherms of $CO_2$, $CH_4$, $O_2$, and $N_2$) in the membrane sample based on polyimide were described using the Dual Mode Sorption model. This model considers the simultaneous sorption of gas in both phases of the membrane material: Henry's law sorption in the polymer matrix and Langmuir-type sorption in the microporous region, referred to as the fractional free volume. A detailed discussion of the various curve-fitting methods is presented in (Tańczyk et al., 2025). In this study, curve fitting was carried out using the least squares method applied to experimental data expressed as $S = f(p)$. In this approach, hereafter referred to as the solubility-based least squares model, each isotherm was approximated by Equation (4), re sulting in a set of coefficients $k_D$, $b$ and $C'_H$ for each gas.

Table 2 also presents the expression ($k_D + C'_H \cdot b$), which, according to Equation (4), represents the maximum solubility at near-zero pressure. It can be observed that the value of this

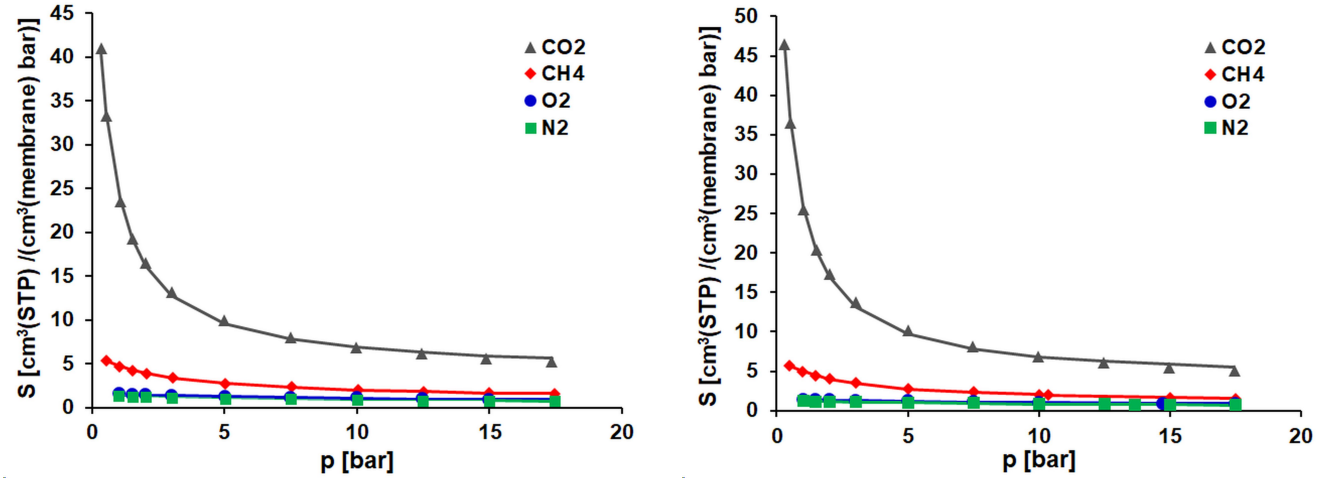


Figure 9. Solubility of pure gases in the polyimide-based membrane from UBE's UMS-A5 module (a) before (a) and (b) after exposure of the membrane to $H_2S$ at 293 K. Points represent experimental data and lines Dual Mode Sorption model predictions.

Table 2. *DMS* model coefficients for the sorption of biogas components in the polyimide-based membrane from the UBE's UMS-A5 module at 293 K. Coefficients were calculated using the *DMS* model with minimized solubility squared differences.

| Gas | $CO_2$ | | $CH_4$ | | $O_2$ | | $N_2$ | |
|---|---|---|---|---|---|---|---|---|
| | before $H_2S$ | after $H_2S$ | before $H_2S$ | after $H_2S$ | before $H_2S$ | after $H_2S$ | before $H_2S$ | after $H_2S$ |
| $k_D$[1] | 3.8715 | 3.7158 | 0.8535 | 0.9096 | 0.4491 | 0.4974 | 0.4424 | 0.2626 |
| $C'_H$[2] | 31.177 | 32.832 | 14.439 | 13.662 | 11.889 | 11.140 | 7.025 | 14.400 |
| $b$[3] | 1.9971 | 2.1333 | 0.3735 | 0.4245 | 0.0993 | 0.0885 | 0.1411 | 0.0696 |
| $k_D + C'_H \cdot b$ | 66.135 | 73.756 | 6.2467 | 6.7090 | 1.6293 | 1.4830 | 1.4337 | 1.2653 |
| *ARE*[4] | 0.227 | 0.271 | 0.099 | 0.139 | 0.041 | 0.184 | 0.071 | 0.027 |
| *SEE*[5] | 0.378 | 0.491 | 0.036 | 0.055 | 0.006 | 0.050 | 0.010 | 0.004 |

[1] $k_D$ [cm³(STP)/(cm³(membrane)·bar)]; [2] $C'_H$ [cm³(STP)/(cm³(membrane))]; [3] $b$ [1/bar]; [4] *ARE* [%];
[5] *SEE* [cm³(STP)/(cm³(membrane)·bar)]

expression increases for carbon dioxide and methane, while it decreases for oxygen and nitrogen after the membrane is exposed to hydrogen sulfide.

The sorption isotherms of $CO_2$, $CH_4$, $O_2$, and $N_2$ determined using the *DMS* model with the coefficients listed in Table 2 are presented graphically (as lines) along with the experimental data points in Figure 8. As shown in this figure, the qualitative agreement between the experimental isotherms and those predicted by the *DMS* model is good for all gases. Quantitative agreement is also satisfactory, as indicated by the low values of the relative error (*ARE*) and the standard error of estimation (*SEE*), which are given in Table 2. These errors are defined by Equations (8) and (9), respectively. The latter was proposed for evaluating the fit quality of the *DMS* model (Ricci and De Angelis, 2019).

Based on the Dual Mode Sorption model for individual gases, it is possible to determine the contribution of sorption both in the polymer matrix and in the free volume of the glassy polymer. The obtained results are presented graphically in Figure 10.

The total solubility of carbon dioxide is approximately 3–7 times higher than that of methane and about 5–15 times higher than the solubility of the other gases. For $CO_2$ and $CH_4$, the contribution of sorption in the Langmuir sites is significant and decreases with increasing pressure. In the pressure range of 0.5–2 bar, it decreases from 89% to 76% for $CO_2$ and from 84% to 78% for $CH_4$, then reaches 31% for $CO_2$ and 46% for $CH_4$ at the maximum pressure. In the case of oxygen and nitrogen, due to weak interactions between gas molecules and the polymer, their concentration in the membrane is very low. The obtained solubility of these gases in the fractional free volume

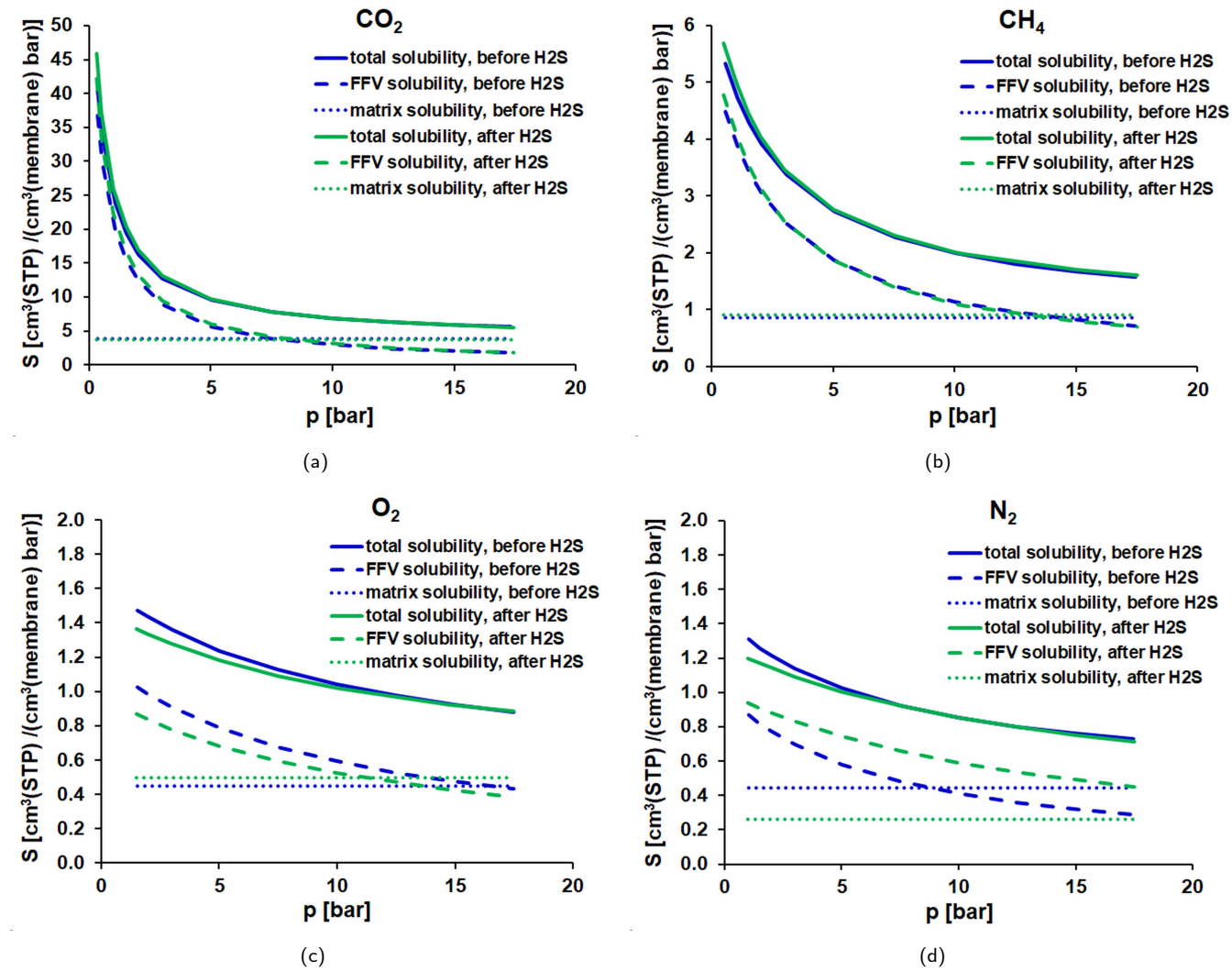


Figure 10. Total and fractional free volume solubility of pure (a) $CO_2$, (b) $CH_4$, (c) $O_2$ and (d) $N_2$ at 293 K established with *DMS* model before and after exposure of the membrane to $H_2S$.

may not reflect reality. For this reason, the results should be approached with great caution. However, it can be stated that exposure of the membrane to hydrogen sulfide does not affect the total solubility of the individual gases. The clearly better affinity of carbon dioxide compared to methane and the other gases during sorption in the *FFV* is expressed by the higher values of the parameter *b*, which are presented in Table 2.

## 3.3. Diffusivity of pure $CO_2$, $CH_4$, $O_2$ and $N_2$

In the solubility-diffusion model, a simple relationship is defined between permeation, solubility, and diffusivity (Equation 1). Knowing any two of these parameters allows the determination of the third. Based on the experimentally determined values of permeation (experimental points in Fig. 6) and solubility of gases in the studied polyimide membrane sample in this work, the diffusion coefficients of all gases in the membrane material were calculated. For the calculation of gas diffusion coefficients, the membrane thickness was assumed to be 1 µm. Their dependence on pressure is graphically presented in Figure 11.

The diffusivity coefficients presented in the graph increase monotonically and almost linearly with rising pressure for each tested gas. At the same time, these coefficients deteriorated by approximately 35–43% for every gas after the membrane's exposure to $H_2S$, which may indicate an antiplasticization effect, as described in (Soroodan Miandoab et al., 2021).

The experimental diffusivity coefficients of all gases were approximated using the partial immobilization model, with the parameters of this model summarized in Table 3.

In the partial immobilization model, the gas diffusion coefficient in the polymer matrix, $D_D$, is the slope coefficient of the straight line, which represents the linearized form of Equation (5), and the ratio of diffusion coefficients in the Langmuir and Henry sorption modes, $F$, can be determined from the intercept, $D_D \cdot K \cdot F$. Table 3 also presents the coefficient of determination $R^2$. It can be observed that for practically every gas, a very good fit of the model to the data was obtained.

Based on Table 3, conclusions can be drawn regarding the mobility of gases in the free volume of the polymer before and

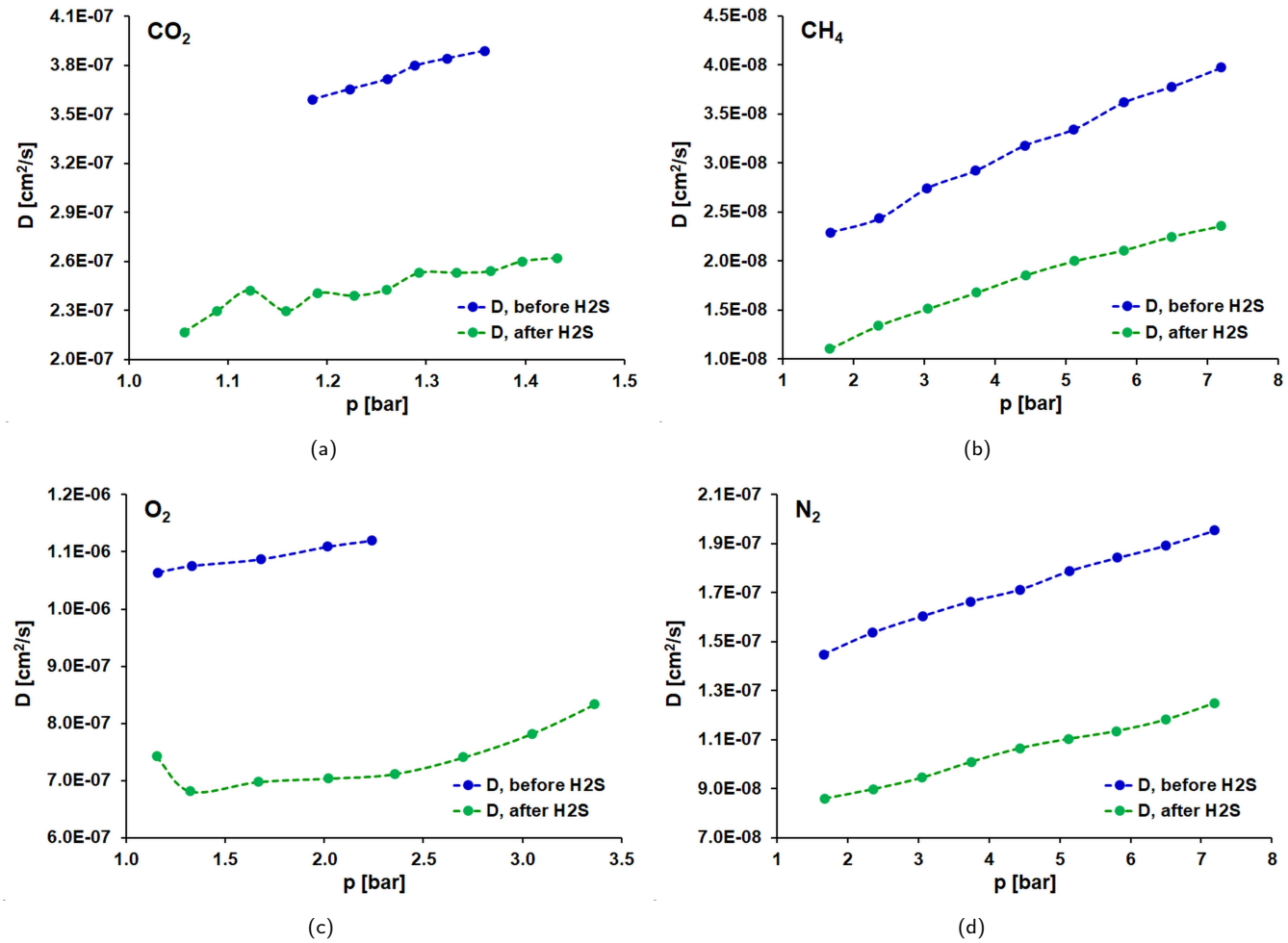


Figure 11. Comparison of diffusivity of pure gases at ambient temperature before and after exposure of the membrane to $H_2S$ for (a) $CO_2$, (b) $CH_4$, (c) $O_2$ and (d) $N_2$.

Table 3. Partial immobilization model coefficients for the sorption and diffusion of biogas components in the polyimide-based membrane from the UBE's UMS-A5 module at 293 K.

| Gas | | $K$ | $D_D$, cm$^2$/s | $F$ | $R^2$ |
|---|---|---|---|---|---|
| $CO_2$ | before $H_2S$ | 16.0823 | $7.35 \cdot 10^{-7}$ | 0.129 | 0.9973 |
| | after $H_2S$ | 18.8495 | $4.65 \cdot 10^{-7}$ | 0.189 | 0.9376 |
| $CH_4$ | before $H_2S$ | 6.3191 | $5.38 \cdot 10^{-8}$ | 0.150 | 0.9986 |
| | after $H_2S$ | 6.3758 | $3.20 \cdot 10^{-8}$ | 0.039 | 0.9997 |
| $O_2$ | before $H_2S$ | 2.6282 | $1.97 \cdot 10^{-6}$ | 0.323 | 0.9980 |
| | after $H_2S$ | 1.9813 | $1.93 \cdot 10^{-6}$ | 0.061 | 0.9610 |
| $N_2$ | before $H_2S$ | 2.2408 | $2.68 \cdot 10^{-7}$ | 0.228 | 0.9996 |
| | after $H_2S$ | 3.8174 | $3.18 \cdot 10^{-7}$ | 0.031 | 0.9975 |

after exposure of the membrane to hydrogen sulfide. It can be observed that only in the case of $CO_2$ does the mobility of this gas in the *FFV* increase from 0.129 to 0.189 in the membrane after exposure to $H_2S$. The mobility of the other gases practically disappears. It decreases from 0.150 to 0.039 for $CH_4$, from 0.323 to 0.061 for $O_2$, and from 0.228 to 0.031 for $N_2$.

It is also worth noting that the diffusion coefficients in the polymer matrix change after the membrane's exposure to $H_2S$. For $CO_2$, $CH_4$, and $O_2$, the diffusion coefficients in the Henry's region decrease by 37% for $CO_2$, 41% for $CH_4$, and 21% for $O_2$. In contrast, for $N_2$, the $D_D$ coefficient increases by 21% in the membrane after exposure to $H_2S$.

It should be noted that the partial immobilization model does not account for phenomena that may accompany $CO_2$ permeation through polymer membranes, such as swelling or plasticization (Kadirkhan et al., 2022; Soroodan Miandoab et al., 2021; Neyertz and Brown, 2020; Ricci et al., 2022). In particular, the coefficient $D_D$ is a constant parameter in this model, and the dependence of the overall diffusion coefficient, $D$, on concentration is captured by the product of the parameter $b$ and pressure. For gases that adsorb strongly (in this case $CH_4$) or very strongly (in this case $CO_2$) in the fractional free volume, the overall diffusion coefficient value should theoretically approach $D_D$.

## 4. CONCLUSIONS

A commercially available glassy polymer membrane UMS-A5 from UBE, based on modified polyimide, was tested for changes in transport properties after exposure to hydrogen sulfide. For this purpose, the permeability of the main biogas components ($CH_4$ and $CO_2$) as well as the most common impurities present in agricultural biogas ($N_2$) and $O_2$) were experimentally determined before and after exposure of the glassy polyimide membrane to $H_2S$. A decrease in permeation coefficients by 30–42% was observed for all gases after membrane exposure to $H_2S$.

To obtain a more comprehensive understanding of the effect of hydrogen sulfide on the membrane, the total solubility of all investigated gases in the polyimide-based membrane was determined using the gravimetric method. Experimental sorption isotherms of all gases were utilized to derive the coefficients of the Dual Mode Sorption model, *DMS*, enabling predictions of gas solubility. The physical reliability of the model coefficients was justified based on their consistency across different data fitting methods and models, as well as good fitting accuracy. Furthermore, the solubility analysis of all gases revealed the dominant contribution of $CO_2$ sorption in the fractional free volume, *FFV*, of the tested polyimide membrane, along with significantly higher solubility of $CO_2$ both in the polymer matrix and in the *FFV*. It was found that exposure of the membrane to hydrogen sulfide did not affect the total solubility of the individual gases.

Based on the solubility of biogas components, calculated from the *DMS* model, as well as the permeability of these gases measured in independent tests, their diffusion coefficients in the tested polyimide membrane sample were determined both before and after membrane exposure to $H_2S$. These diffusivities were described using the partial immobilization model. It was found that $CO_2$ diffusion in the tested glassy polymer sample was an order of magnitude faster than that of $CH_4$. It was also observed that diffusion coefficients in the polymer matrix changed after membrane exposure to $H_2S$. For $CO_2$, $CH_4$ and $O_2$, the diffusion coefficients in the Henry's mode species decreased, whereas for $N_2$ the $D_D$ coefficient increased.

Additionally, it was noted that the mobility of $CO_2$ in the FFV increased only for this gas, while the mobility of the other gases practically vanished in the membrane after exposure to $H_2S$.

The developed methodology for assessing the transport properties of the glassy polymer membrane after exposure to hydrogen sulfide, based on the *DMS* and partial immobilization models, may be useful for evaluating the transport properties of new membrane materials.

## ACKNOWLEDGEMENTS

*The research presented in the work was partially carried out within statutory research funds of the Institute of Chemical Engineering, Polish Academy of Sciences.*

*The research presented in the work was partially carried out within statutory research funds of the Silesian University of Technology.*

## SYMBOLS

| | |
|---|---|
| $A$ | membrane area, $cm^2$ |
| *ARE* | average relative error, % |
| $b$ | Langmuir affinity coefficient, 1/bar |
| $C$ | gas concentration in a polymer, $cm^3(STP)/cm^3$ (membrane) |
| $C_D$ | gas dissolved in the polymer matrix, $cm^3(STP)/cm^3$ (membrane) |
| $C_H$ | gas fraction adsorbed in the fractional free volume, $cm^3(STP)/cm^3$ (membrane) |
| $C'_H$ | Langmuir saturation constant, $cm^3(STP)/cm^3$ |
| $C_{H2S}$ | $H_2S$ concentration in retentate, ppmv |
| $D$ | diffusion coefficient, $cm^2/s$ |
| $D_D$ | diffusion coefficient due to the Henry mode species, $cm^2/s$ |
| $D_H$ | diffusion coefficient due to the Langmuir mode species, $cm^2/s$ |
| *DMS* | Dual Mode Sorption |
| $F$ | dimensionless parameter (see Eq. (7)) |
| $F_{Pi}$ | permeate flow rate, $cm^3/min$ |
| *FFV* | fractional free volume |
| $K$ | dimensionless parameter (see Eq. (6)) |
| $k_D$ | Henry's solubility coefficient, $cm^3(STP)/(cm^3$ (membrane) bar) |
| $n$ | number of experimental points used in the regression |
| $P$ | permeability, $cm^3(STP)/(cm$ (membrane) s bar) |
| $p$ | pressure, bar |
| $R^2$ | coefficient of determination |
| $r$ | number of model parameters |
| $S$ | solubility, $cm^3(STP)/(cm^3$ (membrane) bar) |
| *SEE* | standard error of the estimate, $cm^3(STP)/(cm^3$ (membrane) bar) |

$t$ time, min

$Q$ permeance, $cm^3(STP)/(cm^2(membrane)\ s\ bar)$

$y$ experimental or calculated point

*Greek symbols*

$\alpha$ selectivity

$\delta$ thickness, cm

$\Delta m$ mass change, mg

$\Delta p$ transmembrane pressure drop, bar ($= p_Z - p_P$)

$\delta p$ pressure ratio ($= p_Z/p_P$)

*Subscripts*

*calc* calculations

*D* diffusivity

exp experimental

*i*, *j* number of components

*M* membrane

*P* permeate

*R* retentate

*S* solubility

*Z* feed

## REFERENCES

Ahmad M.Z., Peters T.A., Konnertz N.M., Visser T., Téllez C., Coronas J., Fila V., de Vos W.M., Benes N.E., 2020. High-pressure $CO_2/CH_4$ separation of Zr-MOFs based mixed matrix membranes. *Sep. Purif. Technol.*, 230, 115858. DOI: 10.1016/j.seppur.2019.115858.

Air Liquide, 2024. *Biogas upgrading units*. Available at: https://advancedtech.airliquide.com/markets-solutions/ energy-transition/biogas-upgrading-units.

Air Products Membrane Solutions, 2024. *PRISM® GreenSep LNG*. Available at: https://membranesolutions.com/prism-greensep.

Bahadur I., Osman K., Coquelet C., Naidoo P., Ramjugernath D., 2015. Solubilities of carbon dioxide and oxygen in the ionic liquids methyl trioctyl ammonium bis(trifluoromethylsulfonyl)imide, 1-butyl-3-methyl imidazolium bis(trifluoromethylsulfonyl)imide, and 1-butyl-3-methyl imidazolium methyl sulfate. *J. Phys. Chem. B*, 119, 1503–1514. DOI: 10.1021/jp5061057.

Baker R.W., Low B.T., 2014. Gas separation membrane materials: a perspective. *Macromolecules*, 47, 6999–7013. DOI: 10.1021/ma501488s.

Bos A., Pünt I.G.M., Wessling M., Strathmann H., 1999. $CO_2$-induced plasticization phenomena in glassy polymers. *J. Membr. Sci.*, 155, 67–78. DOI: 10.1016/S0376-7388(98)00299-3.

Cai M., Chen J., Wang H., Wu J., Zhang S., Min Y., 2025. Polyimide-based thermal rearranged (TR) membrane for highly efficient natural gas separation: a review. *Sep. Purif. Technol.*, 355, 129624. DOI: 10.1016/j.seppur.2024.129624.

Fajrina N., Yusof N., Ismail A.F., Aziz F., Bilad M.R., Alkahtani M., 2023. A crucial review on the challenges and recent gas membrane development for biogas upgrading. *J. Environ. Chem. Eng.*, 11, 110235. DOI: 10.1016/j.jece.2023.110235.

Genduso G., Wang Y., Ghanem B.S., Pinnau I., 2019. Permeation, sorption, and diffusion of $CO_2$-$CH_4$ mixtures in polymers of intrinsic microporosity: the effect of intrachain rigidity on plasticization resistance. *J. Membr. Sci.*, 584, 100–109. DOI: 10.1016/j.memsci.2019.05.014.

Harrigan D.J., Lawrence J.A., Reid H.W., Rivers J.B., O'Brien J.T., Sharber S.A., Sundell B.J., 2020. Tunable sour gas separations: simultaneous $H_2S$ and $CO_2$ removal from natural gas via crosslinked telechelic poly(ethylene glycol) membranes. *J. Membr. Sci.*, 602, 117947. DOI: 10.1016/j.memsci.2020.117947.

Hayashi Y., Sugiyama S., Kawanishi T., Shimizu N., 1999. Kinetics of sorption and permeation of water in glassy polyimide. *J. Membr. Sci.*, 156, 11–16. DOI: 10.1016/S0376-7388(98)00273-7.

Houben M., van Geijn R., van Essen M., Borneman Z., Nijmeijer K., 2021. Supercritical $CO_2$ permeation in glassy polyimide membranes. *J. Membr. Sci.*, 620, 118922. DOI: 10.1016/j.memsci.2020.118922.

Hu C.-C., Chang C.-S., Ruaan R.-C., Lai J.-Y., 2003. Effect of free volume and sorption on membrane gas transport. *J. Membr. Sci.*, 226, 51–61. DOI: 10.1016/j.memsci.2003.07.010.

Janusz-Cygan A., Jaschik J., Tańczyk M., 2021. Upgrading biogas from small agricultural sources into biomethane by membrane separation. *Membranes*, 11, 938. DOI: 10.3390/membranes11120938.

Kadirkhan F., Goh P.S., Ismail A.F., Mustapa W.N.F.W., Halim M.H.M., Soh W.K., Yeo S.Y., 2022. Recent advances of polymeric membranes in tackling plasticization and aging for practical industrial $CO_2/CH_4$ applications – a review. *Membranes*, 12, 71. DOI: 10.3390/membranes12010071.

Katariya H.G., Patolia H.P., 2023. Advances in biogas cleaning, enrichment, and utilization technologies: a way forward. *Biomass Conv. Bioref.*, 13, 9565–9581. DOI: 10.1007/s13399-021-01750-0.

Mashhadikhan S., Sanaeepur H., Ebadi Amooghin A., Van der Bruggen B., Shirazian S., 2024. Synthesis of metal-doped covalent triazine frameworks: incorporation into 6FDA-Durene polyimide for $CO_2$ separation through mixed matrix membranes. *J. Environ. Chem. Eng.*, 12, 113965. DOI:10.1016/j.jece.2024.113965.

Neyertz S., Brown D., 2020. Single- and mixed-gas sorption in large-scale molecular models of glassy bulk polymers. Competitive sorption of a binary $CH_4/N_2$ and a ternary $CH_4/N_2/CO_2$ mixture in a polyimide membrane. *J. Membr. Sci.*, 614, 118478. DOI: 10.1016/j.memsci.2020.118478.

Polak D., Szwast M., 2022. Analysis of the influence of process parameters on the properties of homogeneous and heterogeneous membranes for gas separation. *Membranes*, 12, 1016. DOI: 10.3390/membranes12101016.

Pudi A., Rezaei M., Signorini V., Andersson M.P., Baschetti M.G., Mansouri S.S., 2022. Hydrogen sulfide capture and removal technologies: a comprehensive review of recent developments and emerging trends. *Sep. Purif. Technol.*, 298, 121448. DOI: 10.1016/j.seppur.2022.121448.

Ricci E., De Angelis M.G., 2019. Modelling mixed-gas sorption in glassy polymers for $CO_2$ removal: a sensitivity analysis of the Dual Mode Sorption Model. *Membranes*, 9, 8. DOI: 10.3390/membranes9010008.

Ricci E., Minelli M., De Angelis M.G., 2022. Modelling sorption and transport of gases in polymeric membranes across different scales: a review. *Membranes*, 12, 857. DOI: 10.3390/membranes12090857.

Scholes C.A., Tao W.X., Stevens G.W., Kentish S.E., 2010. Sorption of methane, nitrogen, carbon dioxide, and water in Matrimid 5218. *J. Appl. Polym. Sci.*, 117, 2284–2289. DOI: 10.1002/app.32148.

SEPURAN® Green. *Gas separation. A pioneer in biogas upgrading*. Available at: https://www.membrane-separation.com/en/upgrading-of-biogas-to-biomethane-with-sepuran-green.

Sidhikku Kandath Valappil R., Ghasem N., Al-Marzouqi M., 2021. Current and future trends in polymer membrane-based gas separation technology: a comprehensive review. *J. Ind. Eng. Chem.*, 98, 103–129. DOI: 10.1016/j.jiec.2021.03.030.

Soroodan Miandoab E., Kentish S.E., Scholes C.A., 2021. Modelling competitive sorption and plasticization of glassy polymeric membranes used in biogas upgrading. *J. Membr. Sci.*, 617, 118643. DOI: 10.1016/j.memsci.2020.118643.

Suleman M.S., Lau K.K., Yeong Y.F., 2016. Plasticization and swelling in polymeric membranes in $CO_2$ removal from natural gas. *Chem. Eng. Technol.*, 39, 1604–1616. DOI: 10.1002/ceat.201500495.

Tańczyk M., Janusz-Cygan A., Pawlaczyk-Kurek A., Hamryszak Ł., Jaschik J., Janusz-Szymańska K., 2025. Solubility and diffusion of main biogas components in a glassy polysulfone-based membrane. *Molecules*, 30, 614. DOI: 10.3390/molecules30030614.

Tiwari R.R., Jin J., Freeman B.D., Paul D.R., 2017. Physical aging, $CO_2$ sorption and plasticization in thin films of polymer with intrinsic microporosity (PIM-1). *J. Membr. Sci.*, 537, 362–371. DOI: 10.1016/j.memsci.2017.04.069.

Tomczak W., Gryta M., Daniluk M., Żak S., 2024. Biogas upgrading using a single-membrane system: a review. *Membranes*, 14, 80. DOI: 10.3390/membranes14040080.

Tsujita Y., 2003. Gas sorption and permeation of glassy polymers with microvoids. *Prog. Polym. Sci.*, 28, 1377–1401. DOI: 10.1016/S0079-6700(03)00048-0.

UBE Corporation Europe. *UBE $CO_2$ separator for biogas upgrading*. Available at: https://ube.es/products/biogas-upgrading-biomethane-co2-separator.

Werkneh A.A., 2022. Biogas impurities: environmental and health implications, removal technologies and future perspectives. *Heliyon*, 8, e10929. DOI: 10.1016/j.heliyon.2022.e10929.

Wiciak G., Janusz-Cygan A., Janusz-Szymańska K., Tańczyk M., 2021. Determination of the effectiveness of commercial polymeric membranes for carbon dioxide separation. *Desalin. Water Treat.*, 243, 107–115. DOI: 10.5004/dwt.2021.27874.

Wiciak G., Janusz-Szymańska K., Janusz-Cygan A., Pawlaczyk-Kurek A., 2023. Swelling and plasticization of the polymer membrane under the influence of contaminants containing hydrogen sulfide. *Desalin. Water Treat.,* 316, 514–519. DOI: 10.5004/dwt.2023.30167.

Wijmans J.G., Baker R.W., 1995. The solution-diffusion model: a review. *J. Membr. Sci.*, 107, 1–21. DOI: 10.1016/0376-7388(95)00102-I.

Xu S., Zhao N., Wu L., Kang S., Zhang Z., Huo G., Dai Z., Li N., 2022. Carbon molecular sieve gas separation membranes from crosslinkable bromomethylated 6FDA-DAM polyimide. *J. Membr. Sci.*, 659, 120781. DOI: 10.1016/j.memsci.2022.120781.